RSC Advances

PAPER

View Article Online
View Journal | View Issue

Cite this: *RSC Adv.*, 2024, **14**, 29143

Development of a nanocomposite hydrogel catalyzed H_2O_2/TMB system for determination of chlordiazepoxide in exhaled breath condensate

Yasaman Sefid-Sefidehkhan,†[ab] Zahra Karimzadeh,†[c] Abolghasem Jouyban,[a] Maryam Khoubnasabjafari,[de] Vahid Jouyban-Gharamaleki[fg] and Elaheh Rahimpour *[a]

Received 21st May 2024
Accepted 5th September 2024

DOI: 10.1039/d4ra03751k

rsc.li/rsc-advances

In this study, an enzyme mimic catalyzed H_2O_2–tetramethylbenzidine system based on UiO-66/Au NPs–PVA nanocomposite hydrogel was employed as an optical probe for chlordiazepoxide sensing. An excellent detection limit of 0.0032 μg mL^{-1} with a linear range of 0.005–2.0 μg mL^{-1} was obtained for chlordiazepoxide in exhaled breath condensate samples under optimal conditions. The validated system showed good repeatability, simplicity, and stability toward chlordiazepoxide sensing in the exhaled breath condensate of patients receiving this drug.

1. Introduction

Chlordiazepoxide as the first clinically accessible benzodiazepine derivative is a benzodiazepine with anticonvulsant, sedative, antianxiety, and muscle relaxant effects.[1] The chlordiazepoxide metabolic pathway is complicated since the drug is biotransformed into a series of pharmacologically active products including oxazepam, demoxepam, desmethyldiazepam, and desmethylchlordiazepoxide.[2] In healthy people, its distribution volume range is 0.25–0.50 L kg^{-1} and its elimination half-life after a single dose is 5–30 hours.[3] Some techniques for determining chlordiazepoxide documented in the literature include gas chromatography/mass spectrometry,[4] HPLC-UV,[5] adsorptive stripping voltammetry,[6] capillary electrophoresis,[7] and spectrophotometry[8] which all of them have own advantages and disadvantages. However, the development of a sensitive, simple, and accurate procedure for the detection of a drug in a variety of biological matrices is a great challenge for researchers. Different biological samples including urine, plasma, saliva, hair, and exhaled breath condensate (EBC) could be used as biological fluids for chlordiazepoxide sensing.[9–12] EBC is considered a potential substitute biological sample for drug determination[13] and early diagnosis[14] or follow-up procedures due to its simpler matrix than other biological samples. EBC levels of a number of drugs were determined in EBC samples which were reviewed in a recent work.[15]

Nanozymes possessing distinctive physicochemical characteristics and nanomaterials that mimic catalytic activity have attracted significant attention in analytical applications.[16,17] By nanotechnology development in recent years, numerous functional nanomaterials exhibiting catalytic enzyme-like behavior have been discovered. Nanozymes possess unique characteristics such as adjustable catalytic activity based on size (shape, structure, and composition), a large surface area suitable for modification and bio-conjugation, and diverse supplementary functions.[18] Amongst, metal–organic frameworks (MOFs) possess porous topologies and can function as nanozymes due to the presence of metal ions as nodes and organic ligands as linkers. These MOFs can act as biomimetic catalysts independently, utilizing the high-porosity structure of the metal–organic linkers to provide binding sites for substrates within the framework. Due to their larger surface area, increased number of exposed active sites, and reduced diffusion barrier, 2D MOFs demonstrated superior catalytic activities compared to their 3D bulk counterparts. This enhanced performance enables them to offer improved sensitivity for biomolecule sensing.[16,18] Nevertheless, as the time frame of testing increases, a majority of nanoparticles and their hybrids have a tendency to aggregate. In order to address this problem, introducing innovative functional platforms in alternative mediums is needed.[19]

[a]*Pharmaceutical Analysis Research Center and Faculty of Pharmacy, Tabriz University of Medical Sciences, Tabriz, Iran. E-mail: rahimpour_e@yahoo.com*
[b]*Student Research Committee, Faculty of Pharmacy, Tabriz University of Medical Sciences, Tabriz, Iran*
[c]*Research Center for Pharmaceutical Nanotechnology, Biomedicine Institute, Tabriz University of Medical Sciences, Tabriz, Iran*
[d]*Tuberculosis and Lung Diseases Research Center, Tabriz University of Medical Sciences, Tabriz, Iran*
[e]*Department of Anesthesiology and Intensive Care, Faculty of Medicine, Tabriz University of Medical Sciences, Tabriz, Iran*
[f]*Liver and Gastrointestinal Diseases Research Center, Tabriz University of Medical Sciences, Tabriz, Iran*
[g]*Kimia Idea Pardaz Azarbayjan (KIPA) Science Based Company, Tabriz University of Medical Sciences, Tabriz, Iran*
† Sefid-Sefidehkhan and Karimzadeh have equally cooperated as the joint first authors.

Introducing the hydrogel matrix not only stabilized nanomaterials but also enhanced the sensitivity of the system.[20] Therefore, the utilization of porous MOF-based structures in polymeric networks, forming nanocomposite hydrogel could achieve further enhancements.

In many cases, natural enzyme such as horseradish peroxidase was used as a catalyst for speeding up the oxidation of a substrate by H_2O_2. However, they suffer from some serious disadvantages including denaturation by environmental change (such as temperature, pH and *etc.*), high cost and rigorous storage conditions.[21] Recent breakthroughs in the development of nanomaterials have led to the creation of novel nanomaterials with distinctive chemical, physical, and mechanical properties. These nanomaterials have demonstrated exceptional potential as high-efficiency catalysts, exhibiting peroxidase-like activity that can be leveraged in a wide range of applications.[22] Herein, nanocomposite hydrogel based on UiO-66/Au NPs with excellent mechanical properties was fabricated and utilized as an enzyme mimetic. UiO-66/Au NPs embedded hydrogel facilitated the reaction between 3,3,5,5-tetramethyl benzidine (TMB) and H_2O_2 and provided an optical probe for the analysis of chlordiazepoxide in non-invasive biological fluid samples, such as EBC samples. The optimization process was carried out using one-at-a-time technique and experimental design. Once the method was validated, it was applied to the analysis of chlordiazepoxide in the patient EBC samples.

2. Method and materials

2.1. Materials

Sodium borohydride ($NaBH_4$), chloroauric acid ($HAuCl_4$), zirconium chloride ($ZrCl_4$, 98%), acetic acid (HAc, 99.5%), terephthalic acid (H_2BDC, 99%), and *N*,*N*-dimethylformamide (DMF) were purchased from Sigma-Aldrich (USA). Sodium dihydrogen phosphate (NaH_2PO_4), disodium tetraborate decahydrate ($Na_2B_4O_7{\cdot}10H_2O$), TMB, hydrogen peroxide (H_2O_2), ethanol, and polyvinyl alcohol (PVA) were reached from Merck (Germany). Hydrochloric acid and sodium hydroxide were purchased from Scharlau (Barcelona, Spain), and phosphate and acetate buffers were made from sodium dihydrogen phosphate and sodium acetate (Merck) and adjusted at different pHs. Double-distilled deionized water and chlordiazepoxide were attained from Shahid Ghazi Pharmaceutical Company (Tabriz, Iran) and Loghman Pharmaceutical Company (Iran), individually. All the materials were of analytical grade and used without further purification.

2.2. Instruments

A UV-1800 spectrophotometer (Shimadzu, Japan) was used to collect UV-vis absorption spectra. An attenuated total reflection infrared (FT-IR) spectrum was generated using a PerkinElmer (USA) ATR-IR spectrometer. pH measurements were taken with a Metrohm Ltd., Switzerland, digital pH meter model 744 and TEM images were captured with a CM30 (Philips, The Netherlands).

2.3. Synthesis of enzyme mimic UiO-66/Au NPs–PVA hydrogel

An ultrasonic-aided double-solvent technique was used for the synthesis of UiO-66/Au NPS according to previously published works.[23] In detail, 500 mg of synthesized UiO-66 according to the ref. 24, was placed in a 50 mL : 50 mL of ethanol : water ultrasonic bath for 15 minutes. Then, $HAuCl_4$ solution (2.5 mL, 0.025 mol L^{-1}) was added sequentially and constantly stirred for 4 hours at 4 °C. After 30 minutes incubation at 0 °C, $NaBH_4$ (10 mL, 0.05 mol L^{-1}) was slowly dropped. The color of the mixture transitioned from a pale yellow to a pink hue, signifying the formation of UiO-66/Au NPs. To facilitate subsequent examinations, the obtained solution was dried after washing with water. In the following, to synthesize the nanocomposite hydrogel, 10 mL of PVA solution (10% W/V) was directly mixed with 0.1 g UiO-66/Au NPs dispersed in 1 mL of water following the addition of 300 μL borax solution with 5% W/V. After 30 minutes of stirring at 80 °C, the desired nanocomposite hydrogel was synthesized. Before analysis, it was diluted 50 times with water for the experiments.

2.4. Sample preparation

Due to the fact that EBC is a low-protein aqueous and highly diluted matrix, no sample preparation or pretreatment is needed when evaluating the obtained samples. EBC samples were collected using a lab-designed setup[25] and examined without the use of any sample preparation. Calibration and optimization were carried out using samples from healthy volunteers. The EBC samples examined for assessing the effectiveness of the approach were obtained from four patients taking chlordiazepoxide. Prior to the collection, the sample donors (both healthy and patient) provided their consent by signing a form that was validated by the ethical committee of Tabriz University of Medical Sciences with an encryption of IR.TBZMED.VCR.REC.1401.123.

2.5. General procedure

In a 2 mL microtube, a batch analysis procedure was used. After adding 20 μL of phosphate buffer 0.1 mol L^{-1} (pH 5.0) to the microtube containing patient EBC or EBC spiked with standard chlordiazepoxide, 100 μL of UiO-66/Au NPs–PVA nanocomposite hydrogel, 55 μL of TMB (3.0 mmol L^{-1}) and 110 μL H_2O_2 (8.75% v/v) were added and the solution was diluted to 500 μL and incubated for 15 minutes. The analytical response was documented by absorbance measurements at 650 nm.

3. Results and discussion

3.1. Characterization of synthesized nanozyme

The TEM image of UiO-66/Au NPs–PVA nanocomposite hydrogel was provided to characterize the nanoparticles' size and shape. The TEM image of UiO-66 revealed a tetrahedral and octahedral cage with a particle size of ~133.8 ± 11.6 nm by investigating the size distribution histogram. UiO-66 has a porosity-filled tetrahedral and octahedral cage,[26] making it ideal for collecting small metallic NPs. Therefore, the absence

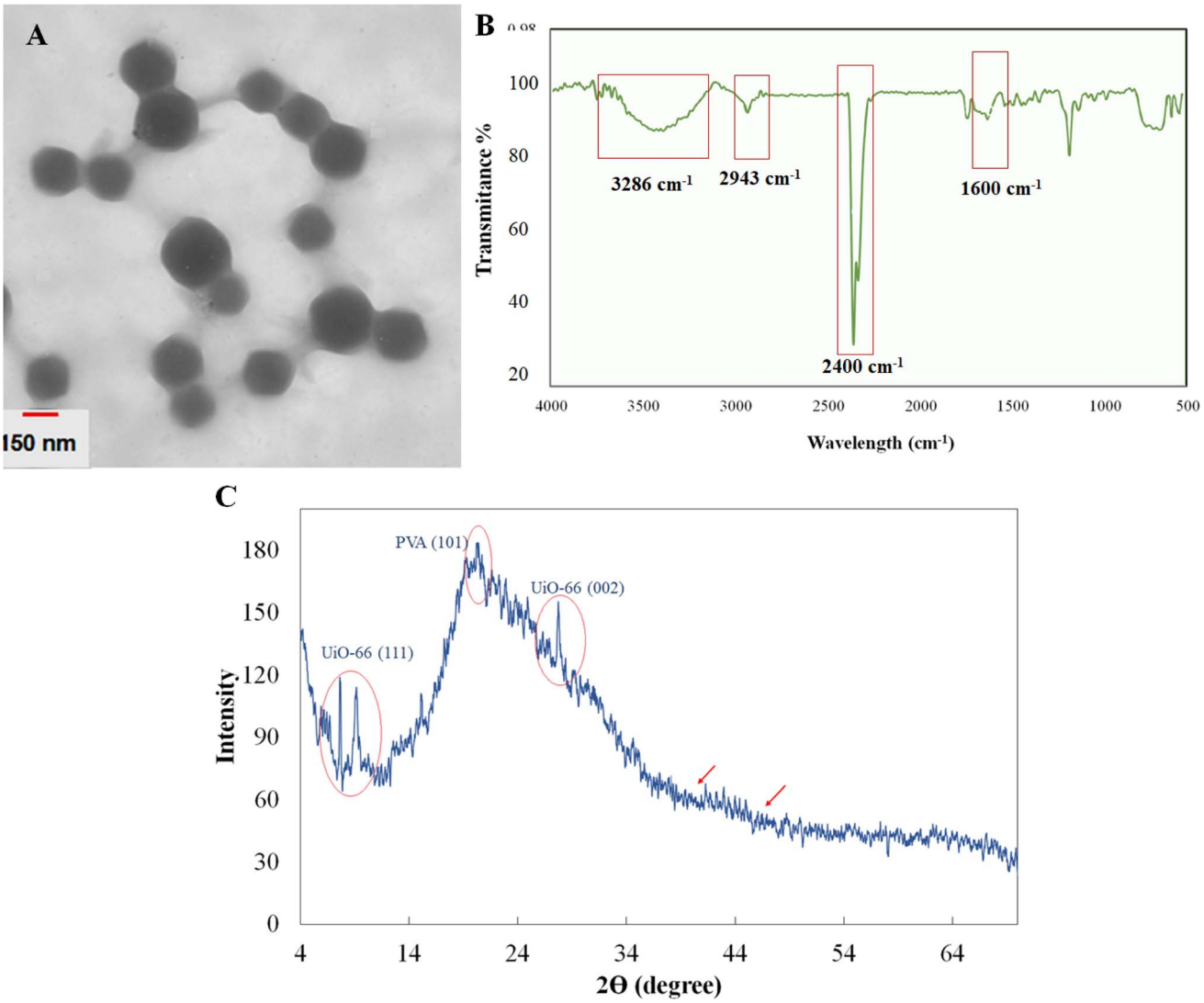

Fig. 1 The TEM image (A), FT-IR spectra (B), and XRD pattern (C) of the synthesized UiO-66/Au NPs–PVA nanocomposite hydrogel.

of AuNPs on UiO-66 in Fig. 1A may indicate that AuNPs have already been trapped in the UiO-66 cages. Also, the crosslinking of polymer-borax could be simply seen between UiO-66 NPs.

To investigate the surface functionalized groups, ATR-FT-IR was also employed. The FT-IR spectra of the generated nanoparticles were revealed in Fig. 1B. Because of the C–O stretching vibration, there were significant absorption bands at approximately 1100–1200 cm^{-1}.[23,27] The additional peak at around 1600 cm^{-1} originates from the organic aromatic linkers in UiO-66.[28] Furthermore, the wider peak at 3286 cm^{-1}, corresponding to the stretching vibration of –OH in PVA, signifies the establishment of intermolecular H-bonding due to cross-linking after the formation of the hydrogel. To verify the phase purity and crystallinity of the synthesized nanozyme, XRD analysis was performed (Fig. 1C). The absence of Au (111) and Au (200) at 2θ = 38.25 and 44.46 suggests that either the AuNPs content was low, and UiO-66's remarkable micropore structure allows for the embedding of NPs within the cavity instead of their physical attachment on the surface according to.[29] Furthermore, the presence of distinct diffraction peaks at $2\theta = 19.8°$ (101) and 20.18 (101) or 22.9 planes can be attributed to the orthorhombic lattice structure of the semi-crystalline nature of the PVA.[30] Even in the composite form of UiO-66/Au NPs–PVA nanocomposite hydrogel, peaks at $2\theta = 7$ and 8 corresponds to (111) and (002) lattice planes of the UiO-66 crystallinity.[31]

3.2. Probe response toward chlordiazepoxide

After ensuring the successful preparation of the synthesized nanozyme, its performance as an enzyme mimetic in H_2O_2 : TMB system has been examined by analyzing the response as a function of the concentration of chlordiazepoxide. When chlordiazepoxide was added to the solution containing H_2O_2 : TMB : UiO-66/Au NPs–PVA nanocomposite hydrogel, the absorbance of the oxidized TMB at 650 nm increased (Fig. 2). TMB itself showed no absorbance or special color in the visible region; however, in the presence of peroxidase or peroxidase mimetic materials, TMB can react with H_2O_2 to produce a colored product. The employed peroxidase mimetic material

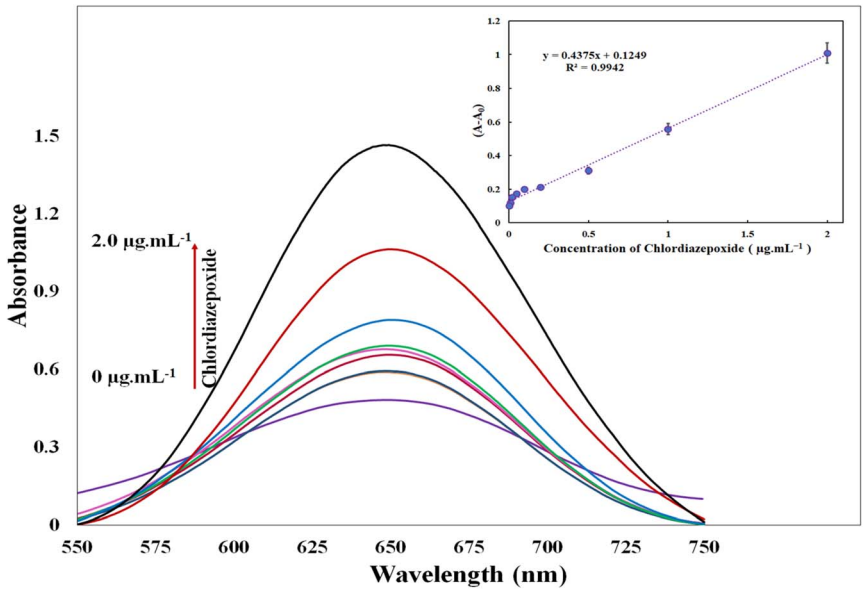

Fig. 2 UV-Vis spectra of the UiO-66/Au NPs–PVA in the absence and presence of chlordiazepoxide at varying concentrations ranging from 0.005 to 2.0 µg mL^{-1} in EBC sample. Inset: calibration plot of UiO-66/Au NPs–PVA nanocomposite hydrogel catalyzed H_2O_2 : TMB system in the presence of chlordiazepoxide in the concentration range of 0.005–2.0 µg mL^{-1} in optimum conditions.

in the current study was UiO-66/Au NPs–PVA nanocomposite hydrogel. An efficient peroxidase mimetic degrades H_2O_2 to OH radicals which can induce the conversion of non-colored TMB to blue-colored oxidized TMB. Fig. 2 showed absorbance spectra under different conditions.

The UiO-66/Au NPs–PVA nanocomposite hydrogel catalyzed TMB–H_2O_2 system was used for the determination of chlordiazepoxide in EBC samples. We suggested that chlordiazepoxide might interact with the peroxidase mimetic activity of the UiO-66/Au NPs–PVA nanocomposite hydrogel, enhancing its ability to catalyze the reaction between TMB and H_2O_2. Chlordiazepoxide has a 7-membered diazepine ring, which contains a nitrogen atom with a lone pair of electrons. This nitrogen atom is part of a benzene ring, which is attached to a benzophenone moiety. The presence of the benzophenone group introduces an electron-withdrawing effect, making the nitrogen atom more electrophilic (electron-accepting).[32] The redox active center in chlordiazepoxide can participate in electron transfer reactions due to its ability to donate or accept electrons. When chlordiazepoxide interacted with the UiO-66/Au NPs–PVA nanocomposite hydrogel, its redox activated center can facilitate electron transfer between the metal centers (Au NPs) and TMB. So that, the chlordiazepoxide molecule can bridge the gap between the metal centers and H_2O_2, and TMB and allowing for efficient electron transfer and facilitating the oxidation reaction. The similar mechanism was previously reported in the literature for enhancing the activity of the enzyme mimics catalysts.[33]

3.3. An experimental design method for optimizing reaction conditions

Diverse reaction parameters such as pH, incubation time, amount of TMB, H_2O_2, and nanozyme have been adjusted to provide the most efficient condition for chlordiazepoxide sensing. For that, the one-at-a-time approach was used to investigate reaction time. The difference in absorbance intensity with and without spiked samples containing 0.05 µg mL^{-1} chlordiazepoxide was used as an analytical response. The results show that the response was enhanced up to 15 minutes (Fig. 3), in which the color of the blank and sample solution vanished and the response decreased.

Furthermore, central composite design (CCD) was used to explore the main affective parameters such as the amount of TMB, H_2O_2, and UiO-66/Au NPs–PVA hydrogel. A CCD was used to consider the correlation between responses and variables. ANOVA analysis was also used to test the validity of the CCD model, the parameters effect, and the interaction between them. R^2 and adjusted-R^2 were used to demonstrate the predictability of the model. Counter plots were used to demonstrate the individual and interaction effects of the parameters on the outcome. Table 1 summarized the coded and related uncoded values for each parameter.

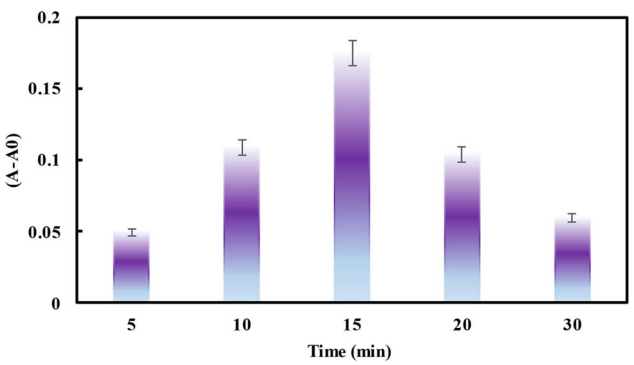

Fig. 3 Effect of time on response of the developed sensor.

Table 1 Coded and actual values of independent variables of the experimental design

	Ranges and levels				
Variables	−2	−1	0	+1	+2
pH (X_1)	3.0	5.0	7.0	9.0	11.0
Amount of nanozyme (μL) (X_2)	25.0	50.0	75.0	100.0	125.0
H_2O_2 : TMB volume ratio (X_3)	(1 : 2)	(1 : 1)	(3 : 2)	(2 : 1)	(5 : 2)

Using 3D surfaces, the impact of selected parameters on the results was illustrated. Fig. 4A clearly shows that the optimal pH for the chlordiazepoxide sensing procedure was 5.0. Another parameter was the concentration of H_2O_2 and TMB as redox reagents. These parameters were investigated as volume ratio of TMB (3.0 mmol L^{-1}) and H_2O_2 (8.75% v/v). The study was performed in the various H_2O_2 : TMB volume ratios. As can be seen, the system response was the highest at ratio of (2 : 1). Therefore, a H_2O_2 : TMB volume a ratio of (2 : 1) was chosen for further actions. Furthermore, the response counterplot for pH and the amount of nanozyme can be found in Fig. 4B. The relationship between pH and the volume of UiO-66/Au NPs–PVA nanocomposite hydrogel was displayed in Fig. 4C. These plots indicate that 100 μL of nanozyme effectively catalyzed the specified amount of TMB and H_2O_2 system.

The ANOVA analysis, the lack of fit tests and residuals of the regression model were investigated and the results were listed in Table 2. Based on the results, an empirical second-order polynomial equation was derived. This equation was formulated in terms of coded factors after eliminating the non-significant factors:

$$Y = 0.2608 - 0.2512X_1 + 0.0280X_2 + 0.0355X_3 + 0.0629X_{12} - 0.0273X_{13} - 0.0215X_{23} + 0.0781X_{11} + 0.0096X_{22} - 0.0159X_{33}$$

In which, Y was the absorbance of the UiO-66/Au NPs–PVA nanocomposite hydrogel catalyzed H_2O_2 : TMB system in the absence and presence of the analyte ($A_0 - A$), and X_1, X_2, and X_3 were the pH, H_2O_2 : TMB volume ratio, and UiO-66/Au NPs–PVA nanocomposite hydrogel volume, individually. Furthermore, the final equation in terms of actual factors was as follows:

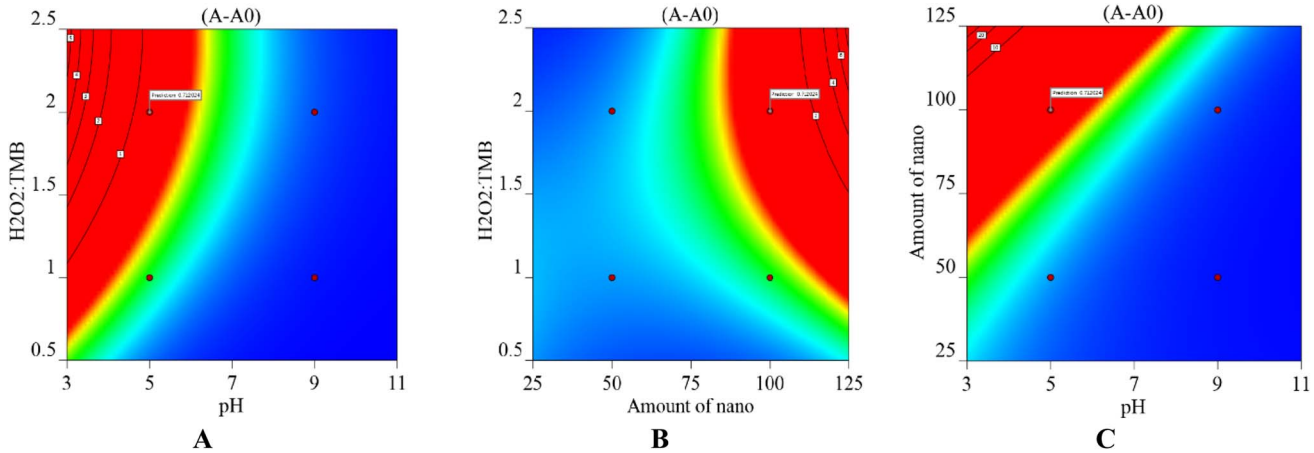

Fig. 4 Counterplots using the quadratic model of $A_0 - A$ against the investigated variable.

Table 2 ANOVA analysis for the response surface quadratic model obtained from CCD

Source	Sum of squares	d*f*	Mean square	*F*-value	*P*-value	
Model	1.25	9	0.1393	18.98	0.0004	Significant
X_1-pH	1.01	1	1.01	137.59	<0.0001	
X_2-amount of nanozyme	0.0126	1	0.0126	1.72	0.2316	
X_3–H_2O_2 : TMB volume ratio	0.0202	1	0.0202	2.75	0.1412	
X_1X_2	0.0316	1	0.0316	4.31	0.0765	
X_1X_3	0.0060	1	0.0060	0.8141	0.3969	
X_2X_3	0.0037	1	0.0037	0.5029	0.5012	
X_1^2	0.1182	1	0.1182	16.11	0.0051	
X_2^2	0.0018	1	0.0018	0.2426	0.6374	
X_3^2	0.0049	1	0.0049	0.6653	0.4416	
Residual	0.0514	7	0.0073			
Lack of fit	0.0429	5	0.0086	2.02	0.3636	Not significant
Pure error	0.0085	2	0.0042			
R^2	0.9606					
Adjusted R^2	0.9100					
Predicted R^2	0.7257					

$$Y = 2.02969 - 0.452354X_1 - 0.007404X_2 + 0.581657X_3 + 0.001258X_{12} - 0.027325X_{13} - 0.001718X_{23} + 0.019531X_{11} + 0.000015X_{22} - 0.063502X_{33}$$

Table 2 shows that R^2 was 0.9606 and adjusted R^2 was 0.9100 demonstrating the significant correlation between the predicted and experimental models.

3.4. Analytical figures of merit

In the investigation of model linearity, a range of standard chlordiazepoxide concentrations in EBC samples were prepared and evaluated in optimum conditions. A linear correlation, with a correlation coefficient of 0.9942, was found between the increasing absorbance signal and the amount of chlordiazepoxide concentrations in the range of (the lowest and highest concentration at which the response is still linear) 0.005–2.0 μg mL^{-1} (inset Fig. 2) using the spectrophotometry method.

The regression equation was $\Delta A = 0.4375C + 0.1249$, where ΔA represents the analytical response obtained by subtracting the absorbance intensity in the absence and presence of chlordiazepoxide in which C denotes the concentration of chlordiazepoxide in μg mL^{-1}. The detection limit of the method was found 0.0032 μg mL^{-1}, calculated as 3 times the ratio of the standard deviation of the blank (S_b) to the slope of the calibration curve (m). The precision of repeatability and reproducibility for a chlordiazepoxide concentration of 0.05 μg mL^{-1} using the relative standard deviations (RSD) of replicated measurements ($n = 5$) was found to be 4.3% and 8.2%, respectively.

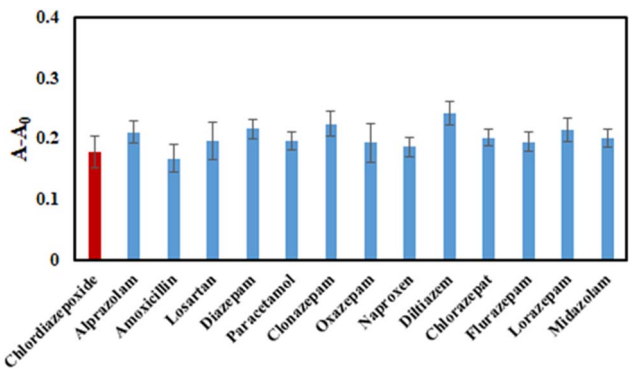

Fig. 5 The interferences study of the proposed probe by employing various potential co-administered or over-the-counter medications at concentrations of 0.05 μg mL^{-1}.

3.5. Investigation of interferences

In order to assess the specificity of the proposed method towards chlordiazepoxide, the investigation was carried out under optimal conditions in the presence of other co-administered or over-the-counter medications. The impact of each pharmaceutical, at concentrations 5 times higher than the target analyte, on the response signal of the system was analyzed. The variation in response in the presence of chlordiazepoxide was measured and summarized in Fig. 5. It was evident from the results that the tested compounds do not significantly affect the probe response. These findings designate an excellent selectivity for accurately determining chlordiazepoxide.

3.6. Comparison of the present method with other reported methods

A comparison between the recent system and other approaches was reported in Table 3. It provides a summary of the analytical features of each method, giving an insight into their capabilities for determining chlordiazepoxide. It was evident that the present method has comparable and satisfactory ability in comparison to the other methods.

3.7. Real sample analysis

The validated method was utilized to quantify chlordiazepoxide in EBC of four patients receiving therapeutic doses of chlordiazepoxide to assess the practicality of the method on actual samples. A summary of the findings was presented in Table 4. In order to assess the accuracy of the method, the recovery calculation was performed by spiking a known and consistent amount of chlordiazepoxide to the analyzed EBC samples. The recovery for the spiked samples was ranged from 95% to 111%,

Table 3 The comparison of the recent system and other reported approaches

Method	Sample	LOD (μg mL^{-1})	Linear range (μg mL^{-1})	Reference
GC-NCIMS[a]	Mouse plasma	0.001	0–0.01	34
DLLME-HPLC-UV	Water, urine, plasma	0.0005	0.005–10	35
Capillary zone electrophoresis	Capsules	0.097	1–100	36
HPLC-UV	Water, urine, plasma	0.0014	0.006–10	37
Adsorptive voltammetry	Pharmaceutical formulation, human serum	0.0168	0.067–1.68	38
Spectrophotometry	Pharmaceutical formulation	2.2802	35–70	39
Spectrofluorimetry	Urine, plasma	—	0.25–6.0	40
Spectrofluorimetry	Blood	—	0.2–3	41
Spectrophotometry	EBC	0.0032	0.005–2.0	This work

[a] Gas chromatographic-negative-ion chemical ionization mass spectrometric.

Table 4 Determination of chlordiazepoxide in real samples

No.	Gender	Age (year)	Co-administered drugs	Added (μg mL^{-1})	Found (μg mL^{-1})	Recovery[a] (%)
1	Male	44	—	—	0.054	—
				0.01	0.063	90.0
				0.05	0.109	110.0
				0.2	0.261	103.5
2	Female	39	Valproate sodium, inderal, biperiden, perphenazine	—	0.042	—
				0.01	0.053	110.0
				0.05	0.094	104.0
				0.2	0.251	104.5
3	Female	41	Depakene, olanzapine	—	0.024	—
				0.01	0.034	100
				0.05	0.080	112.0
				0.2	0.233	104.5
4	Male	34	Codeine	—	0.036	—
				0.01	0.044	80.0
				0.05	0.085	98.0
				0.2	0.241	102.5

[a] Recovery (%) = [(found − base)/added] × 100. "Base" and "Found" refer to the amount of the analyte in samples before and after spiking, respectively.

confirming the accuracy of the method for chlordiazepoxide analysis in the EBC of patient samples.

4. Conclusions

In the current study, a TMB–H_2O_2 system catalyzed by UiO-66/Au NPs–PVA nanocomposite hydrogel has been developed for fast, selective, sensitive, and accurate determination of chlordiazepoxide in EBC samples. Notably, the PVA hydrogel serves as a great platform for simply incorporating UiO-66/Au NPs within the network of PVA. Regarding the results, the absorbance of the redox system gradually increases with increasing chlordiazepoxide concentration. So, this system has the potential to visualize the changes in concentration-dependent absorbance in biological samples such as EBC from patients receiving chlordiazepoxide, yielding satisfactory outcomes (low LOD and wide high linearity) in a short time.

Data availability

The datasets used and/or analysed during the current study are available from the corresponding author on reasonable request.

Author contributions

Yasaman Sefid-Sefidehkhan: investigation. Zahra Karimzadeh: investigation, Abolghasem Jouyban: supervision, writing – review & editing, Maryam Khoubnasabjafari: collecting the real samples, Vahid Jouyban-Gharamaleki: the device managing. Elaheh Rahimpour: data curation, writing – review & editing.

Conflicts of interest

The authors declare no conflict of interest.

Acknowledgements

This work was supported by Research Affairs of Tabriz University of Medical Sciences, under grant number 69783.

References

1 H. M. Al-Kuraishy, *et al.*, Insights on benzodiazepines' potential in Alzheimer's disease, *Life Sci.*, 2023, 121532.
2 F. López-Muñoz, *et al.*, The discovery of chlordiazepoxide and the clinical introduction of benzodiazepines: half a century of anxiolytic drugs, *Anxiety Disord.*, 2011, **25**, 554–562.
3 D. J. Greenblatt, *et al.*, Clinical pharmacokinetics of chlordiazepoxide, *Clin. Pharmacokinet.*, 1978, **3**, 381–394.
4 H. Inoue, *et al.*, Screening and determination of benzodiazepines in whole blood using solid-phase extraction and gas chromatography/mass spectrometry, *Forensic Sci. Int.*, 2000, **113**, 367–373.
5 F. Laffafchi, *et al.*, Creatine@SiO2@Fe3O4 nanocomposite as an efficient sorbent for magnetic solid-phase extraction of escitalopram and chlordiazepoxide from urine samples through quantitation via HPLC–UV, *J. Sep. Sci.*, 2022, **45**, 3005–3013.
6 E. Lorenzo and L. Hernandez, Adsorptive stripping voltammetry of chlordiazepoxide at the hanging mercury drop electrode, *Anal. Chim. Acta*, 1987, **201**, 275–280.
7 Y. Suzuki, *et al.*, The capillary electrophoresis separation of benzodiazepine drug using dextran sulfate and SDS as running buffer, *Biomed. Chromatogr.*, 2004, **18**, 150–154.
8 M. Walash, *et al.*, Spectrophotometric determination of chlordiazepoxide and nitrazepam, *Talanta*, 1988, **35**, 895–898.
9 S. Khodadoust, *et al.*, Solid-phase extraction of losartan and chlordiazepoxide from biological samples using sponge-activated carbon, *Sep. Sci. Plus*, 2024, **7**, 2300096.

10 F. Laffafchi, *et al.*, Creatine@SiO2@Fe3O4 nanocomposite as an efficient sorbent for magnetic solid-phase extraction of escitalopram and chlordiazepoxide from urine samples through quantitation via HPLC–UV, *J. Sep. Sci.*, 2022, **45**, 3005–3013.
11 J. Kim, *et al.*, Validation of a simultaneous analytical method for the detection of 27 benzodiazepines and metabolites and zolpidem in hair using LC-MS/MS and its application to human and rat hair, *J. Chromatogr. B*, 2011, **879**, 878–886.
12 K. Persona, *et al.*, Analytical methodologies for the determination of benzodiazepines in biological samples, *J. Pharm. Biomed. Anal.*, 2015, **113**, 239–264.
13 M. Khoubnasabjafari, *et al.*, Exhaled breath condensate as an alternative sample for drug monitoring, *Bioanalysis*, 2018, **10**, 61–64.
14 S. Kazeminasab, *et al.*, Exhaled breath condensate efficacy to identify mutations in patients with lung cancer: a pilot study, *Nucleos Nucleot.*, 2022, **41**, 370–383.
15 N. Hashemzadeh, *et al.*, Applications of exhaled breath condensate analysis for drug monitoring and bioequivalence study of inhaled drugs, *J. Pharm. Pharm. Sci.*, 2022, **25**, 391–401.
16 J. Wu, *et al.*, Nanomaterials with enzyme-like characteristics (nanozymes): next-generation artificial enzymes (II), *Chem. Soc. Rev.*, 2019, **48**, 1004–1076.
17 A. Jouyban and R. Amini, Layered double hydroxides as an efficient nanozyme for analytical applications, *Microchem. J.*, 2021, **164**, 105970.
18 M. Bilal, *et al.*, Enzyme mimic nanomaterials as nanozymes with catalytic attributes, *Colloids Surf., B*, 2023, **221**, 112950.
19 A. Jouyban and A. Samadi, A Study on Surfactant Solutions as Stop Solution for Metal Nanoparticles Aggregation-Based Colorimetric Assays, *Int. J. Nanosci.*, 2022, **21**, 2250026.
20 M. Zhou, *et al.*, Ratiometric fluorescence sensor for Fe3+ ions detection based on quantum dot-doped hydrogel optical fiber, *Sens. Actuators, B*, 2018, **264**, 52–58.
21 J. Xie, *et al.*, Analytical and environmental applications of nanoparticles as enzyme mimetics, *Trac. Trends Anal. Chem.*, 2012, **39**, 114–129.
22 J. Yun, B. Li and R. Cao, Positively-charged gold nanoparticles as peroxidiase mimic and their application in hydrogen peroxide and glucose detection, *Chem. Commun.*, 2010, **46**, 8017–8019.
23 J. Yang, *et al.*, Highly dispersed AuPd alloy nanoparticles immobilized on UiO-66-NH2 metal-organic framework for the detection of nitrite, *Electrochim. Acta*, 2016, **219**, 647–654.
24 M. Wang, *et al.*, Bimetallic NiCo metal-organic frameworks for efficient non-Pt methanol electrocatalytic oxidation, *Appl. Catal., A*, 2021, **619**, 118159.
25 M. K. Jouyban, K. Ansarin and V. Jouyban-Gharamaleki, Breath Sampling Setup, *Iran Pat.*, 81363, 2013.
26 J. Feng, *et al.*, Hydrogenation of levulinic acid to γ-valerolactone over Pd@ UiO-66-NH2 with high metal dispersion and excellent reusability, *Microporous Mesoporous Mater.*, 2020, **294**, 109858.
27 A. M. Al-Enizi, *et al.*, Synthesis of NiOx@ NPC composite for high-performance supercapacitor via waste PET plastic-derived Ni-MOF, *Compos. B Eng.*, 2020, **183**, 107655.
28 Z. Karimzadeh, *et al.*, A follow-up study on "A sensitive determination of morphine in plasma using AuNPs@UiO-66/PVA hydrogel as an advanced optical scaffold", *Heliyon*, 2023, **9**, e15267.
29 Z. Karimzadeh, *et al.*, Dual-emission ratiometric fluorescent probe based on N-doped CQDs@UiO-66/PVA nanocomposite hydrogel for quantification of pethidine in human plasma, *Microchim. Acta*, 2023, **190**, 128.
30 Y.-N. Chen, *et al.*, Poly(vinyl alcohol)–tannic acid hydrogels with excellent mechanical properties and shape memory behaviors, *ACS Appl. Mater. Interfaces*, 2016, **8**, 27199–27206.
31 S. Govindaraju, *et al.*, Photoluminescent AuNCs@ UiO-66 for ultrasensitive detection of mercury in water samples, *ACS Omega*, 2018, **3**, 12052–12059.
32 J. Conradie, Reduction potential of benzophenones, hydroxyphenones and bis (2-hydroxyphenone) copper molecules, *Electrochim. Acta*, 2023, **443**, 141931.
33 H. Geng, *et al.*, Boosting the peroxidase-like activity of Pt nanozymes by a synergistic effect of Ti3C2 nanosheets for dual mechanism detection, *Dalton Trans.*, 2022, **51**, 11693–11702.
34 D. Song, *et al.*, Determination of chlordiazepoxide in mouse plasma by gas chromatography—negative-ion chemical ionization mass spectrometry, *J. Chromatogr. B*, 1994, **660**, 95–101.
35 S. Khodadoust and M. Ghaedi, Optimization of dispersive liquid–liquid microextraction with central composite design for preconcentration of chlordiazepoxide drug and its determination by HPLC-UV, *J. Sep. Sci.*, 2013, **36**, 1734–1742.
36 S. M. Mohyeldin, *et al.*, AGREE, hexagonal and whiteness assessment approaches for evaluating two novel analytical methods; capillary zone electrophoresis and spectrophotometric assays for simultaneous determination of pantoprazole, chlordiazepoxide, and clidinium bromide ternary mixtures, *Sustain. Chem. Pharm.*, 2023, **33**, 101108.
37 F. Momtazan, *et al.*, Synthesis of mesoporous silica for adsorption of chlordiazepoxide and its determination by HPLC: experimental design, *J. Sep. Sci.*, 2019, **42**, 3253–3260.
38 G. El-Sayed, *et al.*, Adsorptive voltammetric determination of chlordiazepoxide in pure and dosage forms, *J. Chem. Pharm. Res*, 2009, **1**, 225–232.
39 T. A. Al-Samarrai and K. F. Al-Samarrai, Spectrophotometric determination of chlordiazepoxide with 2-(chloromethyl)-5-methyl-1H-benzo[d]imidazole reagent, *AIP Conf. Proc.*, 2022, **2394**, 040050.
40 J. T. Stewart and J. L. Williamson, Fluorometric determination of chlordiazepoxide in dosage forms and biological fluids with fluorescamine, *Anal. Chem.*, 1976, **48**, 1182–1185.
41 J. H. Riddick, An ultraviolet and visible spectrophotometric assay method for chlordiazepoxide, *Clin. Biochem.*, 1973, **6**, 189–199.